Rheological properties and percolation in suspensions of multiwalled carbon nanotubes in polycarbonate

Abbasi, Samaneh; Carreau, Pierre J.; Derdouri, Abdessalem; Moan, Michel

Publisher's version / Version de l'éditeur:
https://doi.org/10.1007/s00397-009-0375-7
Rheologica Acta, 48, 9, pp. 943-959, 2009-07-17

Rheol Acta (2009) 48:943–959
DOI 10.1007/s00397-009-0375-7

ORIGINAL CONTRIBUTION

Rheological properties and percolation in suspensions of multiwalled carbon nanotubes in polycarbonate

Samaneh Abbasi · Pierre J. Carreau · Abdessalem Derdouri · Michel Moan

Received: 22 January 2009 / Accepted: 27 June 2009 / Published online: 17 July 2009

Abstract This paper is concerned with several issues related to the rheological behavior of polycarbonate/multiwalled carbon nanotube nanocomposites. The composites were prepared by diluting a masterbatch of 15 wt.% nanotubes using melt-mixing method, and the dispersion was analyzed by SEM, TEM, and AFM techniques. To understand the percolated structure, the nanocomposites were characterized via a set of rheological, electrical, and thermal conductivity measurements. The rheological measurements revealed that the structure and properties were temperature dependent; the percolation threshold was significantly lower at higher temperature suggesting stronger nanotube interactions. The nanotube networks were also sensitive to the steady shear deformation particularly at high temperature. Following preshearing, the elastic modulus decreased markedly suggesting that the nanotubes became more rigid. These results were analyzed using simple models for suspensions of rod-like particles. Finally, the rheological, electrical, and thermal conductivity percolation thresholds were compared. As expected, the rheological threshold was smaller than the thermal and electrical threshold.

Keywords Multiwalled carbon nanotube · Polycarbonate · Suspension · Rheological percolation · Electrical percolation · Thermal conductivity percolation · Filled polymer · Storage modulus

S. Abbasi · P. J. Carreau (✉)
CREPEC, Department of Chemical Engineering,
Ecole Polytechnique Montreal, P.O. Box 6079,
Station Centre-Ville Montreal QC,
Canada H3C3A7
e-mail: pcarreau@polymtl.ca

A. Derdouri
CREPEC, Industrial Materials Institute,
National Research Council Canada,
75 de Mortagne, Boucherville, QC, Canada

M. Moan
Université de Bretagne Occidentale,
3 rue des Archives-CS 93837-F29238
Brest cedex3, France

Introduction

During the progressive advances in nanoscience and nanotechnology of the last two decades, many scientists have developed a strong interest in the unique properties of novel solid-state nanomaterials, called carbon nanotubes (CNT). Since their discovery in 1991 by Iijima (Iijima 1991; Iijima and Ichihashi 1993), CNTs became attractive candidates for fundamental investigations, and an extensive research effort has been devoted to their fabrication, characterization, and development of applications due to their unique electronic structure and extraordinary properties (Meyyappan 2005). Their intrinsic structure, size scale, and aspect ratio suggest a variety of applications such as nanoelectronics, sensors, and field emission as well as high performance nanocomposites. They exist as single wall carbon nanotube (SWCNT) or multiwall wall carbon nanotube (MWCNT). A SWCNT is made by wrapping a graphene layer into a cylinder. Each tube is represented by its chiral vector, C_h, which is a pair of indices (n,m) with values depending on the way the graphene sheet is wrapped (Meyyappan 2005). Carbon

nanotubes have been recognized among the strongest known materials. For instance, measured values of tensile strength were found to be as high as 63 GPa for a MWCNT (Yu et al. 2000) and extremely high elastic modulus, on the order of 1 TPa, have been proven by both simulation and experimental measurements (Salvetat et al. 1999; Yu et al. 2000). These reported strengths are 10 to 100 times higher than the strongest carbon steel with a tensile strength of approximately 1.2 GPa. Considering the low density of carbon nanotubes, which is in the range of 1.3–1.4 g/mL, their specific strength is the best of known materials. Although carbon nanotubes generally have exceptional properties, the wide ranges of their special applications are mainly related to their unique electrical properties. For a given nanotube, if its chiral vector is represented with $n = m$, the nanotube is metallic; the tube is semiconducting if $n - m$ is a multiple of 3; otherwise, it is a moderate semiconductor (Meyyappan 2005). Based on theoretical calculations, the electrical current density of an individual carbon nanotube can be more than several tim es greater than that of metals such as silver and copper (Breuer and Sundararaj 2004; Xie et al. 2005). CNTs also have excellent thermal conductivity in the range of 3,000 W/m K for individual MWCNTs (Hone 2004).

Recently, considerable attention has been devoted to carbon nanotube/polymer composites owing to their extraordinary properties from both processing and application points of view. Besides the individual properties of carbon nanotubes, a number of potential benefits are expected when they are employed as reinforcing agents in nanocomposites. However, the efficiency of nanotubes to live up to their theoretical potential depends on a good dispersion within the host polymer. At the moment, three methods are commonly used to incorporate nanotubes into a polymer: solution mixing and film casting of suspensions of nanotubes in dissolved polymers, in situ polymerization of nanotube–polymer monomer mixture, and mixing of nanotubes in molten polymers. Melt mixing is the industrially preferred method in many cases because of its environmentally benign character, its versatility, and its compatibility with current polymer processing techniques.

Polycarbonate (PC), a typical amorphous polymer, is an important commercially available engineering thermoplastic for injection molding applications because of its excellent process ability and mechanical properties. Recently, carbon nanotubes have been used as special filler to be incorporated into PC for stiffness reinforcement as well as thermal and electrical conductivities enhancement purposes (Ding et al. 2003; Singh et al. 2003; Potschke et al. 2004a; Pham et al. 2008).

The rheological properties of polymer nanocomposites including viscoelastic (time or frequency- and temperature-dependent) behavior are of practical importance in relation to processing and characterizing the composite microstructure. The rheological behavior depends on the material microstructure, the state of the nanotubes dispersion, the aspect ratio and orientation of the nanotubes, the interaction between nanotubes and polymer chains as well as nanotube–nanotube interactions. The temperature not only influences the rheological properties of the matrix but it also can affect the state of dispersion of the nanocomposites via changes in the particle–particle interactions and in the wettability of the nanotubes with the matrix.

If considerable research has been conducted regarding the physical properties of nanocomposites, including mechanical properties and electrical conductivity, only a few investigations have focused on the rheological behavior of polymer/carbon nanotube nanocomposites. Most of the rheological studies have concentrated on the typical linear viscoelastic response and on the non terminal character at low frequencies, which is attributed to the formation of a filler network (Kharchenko et al. 2004; Meincke et al. 2004; Abdel-Goad and Potschke 2005; Xinfeng et al. 2005; Hu et al. 2006; Moniruzzaman and Winey 2006; Sung et al. 2006; Wu et al. 2007a). To our knowledge, this low frequency behavior was reported first by Potschke et al. in 2002. Since then, more attention has been paid to rheological properties of CNTs/polymer nanocomposites with focus on the percolation threshold as one of the most important factors affecting the material properties or as a characterization parameter of the dispersion quality. Such a percolated system was studied using polyamide-6/MWCNT nanocomposites (Meincke et al. 2004), polycarbonate/MWCNT composites (Abdel-Goad and Potschke 2005), polycarbonate/functionalized MWCNT nanocomposites (Sung et al. 2006), and poly(ethylene terephthalate)/MWCNT (Hu et al. 2006). Finally, a few investigations on the modeling of the rheological behavior of carbon nanotubes suspended in low molecular weight polymeric resins have been recently carried out (Rahatekar et al. 2006; Fan and Advani 2007; Hong and Kim 2007; Ma et al. 2008).

The rheological behavior of nanocomposites strongly depends on the carbon nanotube alignment as well. For example, it was found that the storage modulus G' that describes the elastic response decreases with the alignment of nanotubes. When nanotubes are aligned in the polymer matrix, the probability of tube–tube contacts decreases, and the nanotube network is less effective at impeding the polymer

motion (Du et al. 2004; Wu et al. 2007b). It is also found that the percolated nanotube network is very sensitive to the temperature (Potschke et al. 2004b; Wu et al. 2007a).

In this work, we examined the rheological behavior of PC/MWCNT nanocomposites in light of interactions between CNTs and polymer chains or between CNTs themselves. This is a quite complex and difficult system to study since the typical behavior of polymeric systems almost vanishes in the presence of a nanotube network. For example, as soon as the nanotube network is formed, the low frequency terminal zone observed for the neat polymer disappears. Furthermore, the high temperature behavior adds another complexity to this difficult system. Therefore, typical analysis methods used for conventional polymeric systems are not useful in this context, and a more innovative investigation is required to establish the relationship between the rheological behavior and microstructure of such a system. More specifically, the investigation of the effect of nanotube loading, nanotube alignment, and temperature on the rheological behavior of the nanocomposites was the main objective of this study. The nanocomposite preparation was optimized using various characterization methods. As nanotubes intertwine into agglomerates that are difficult to disperse, we used premixed polymer/carbon nanotube masterbatches and diluted them to the required concentrations by adding the base polymer. This insured consistent and reproducible results. The relationship between the rheological properties and the microstructure is also discussed in light of electrical and thermal conductivity of the nanocomposites.

Experimental

Materials

A masterbatch of 15 wt.% MWCNT in PC was purchased from Hyperion Catalysis International, Cambridge, MA. According to the supplier, the carbon nanotubes are vapor-grown and typically consist of 8–15 graphite layers wrapped around a hollow 5-nm core (Potschke et al. 2002). The diameter range was stated to vary from 15 to 50 nm, and the length ranged between 1 and 10 μm as was confirmed by transmission electron microscopy (TEM) characterization. The masterbatch was diluted with polycarbonate (Calibre 1080) supplied by DOW Chemical to prepare nanocomposite samples of various loadings. Its glass transition temperature (T_g) was determined by DSC measurements and found to be equal to about 145°C.

Nanocomposite preparation

The composites were produced by melt mixing the masterbatch with the neat PC. Prior to mixing, all materials were dried for a minimum of 4 h at 120°C. Six different suspensions with MWCNT contents between 0.2 and 5 wt.% were prepared using a Brabender internal mixer at 50 rpm during 16 min and for two different temperatures, 210°C and 250°C (conditions previously optimized via controlled experiments).

Morphological characterization

The morphology of nanocomposites was studied at room temperature through scanning and transmission electron microscopy (SEM and TEM), and atomic force microscopy (AFM). For SEM, we used the high-resolution Hitachi S-4700 microscope, while for AFM, we utilized the multimode VEEECO scanning probe in tapping mode. Both SEM and AFM were done on ultramicrotomed surfaces of samples that were cut with a diamond knife at room temperature. SEM samples were coated with a vapor deposit of Pt for 25 s. TEM was done on ultrathin sections of nanocomposites using a Hitachi HD-2000 microscope.

Rheological measurements

All the rheological measurements were carried out using a stress-controlled rheometer (CSM rheometer of Bohlin Instruments) equipped with a 25-mm parallel plate geometry under nitrogen atmosphere. Prior to measurements, the compression molded samples were dried for a minimum of 4 h at 120°C. The viscoelastic properties of nanocomposites were investigated in a broad range of temperature from 210°C up to 300°C. Small amplitude oscillatory shear (SAOS) frequency sweep tests were carried out between 0.06 and 200 rad/s in the linear viscoelastic regime. This regime was established in the standard way by measuring the modulus at constant frequency (10 rad/s) and increasing strain magnitude. Further, long-time measurements (up to 3 h) were conducted to investigate the thermal stability of the nanocomposite samples. We assumed that the particle sizes were sufficiently small compared to the gap; however, the absence of apparent slip at the wall has been ascertained by varying the gap from 0.5 to 1.5 mm. The differences were found to be insignificant, less than the reproducibility of the data estimated to be within 3.5% for all the frequency sweep tests conducted with the various nanotube loadings.

In addition, the effect of high shear on the microstructure of the nanocomposites was evaluated by

subjecting each sample to different levels of constant shear stress for various periods of time. SAOS measurements were then performed without any rest time between the preconditioning step and the frequency sweep test.

Electrical resistivity measurements

The volume resistivity of the PC/MWCNT nanocomposite samples was determined by measuring the DC resistance across the thickness of compression molded disks using a Keithley electrometer model 6517 equipped with a two probe test fixture. We used a specific kind of test fixture firmly connected to the probes. All the connections were made using short wires to assure that the resistivity of the whole setup was negligible. The resistivity of the setup was measured each time before the tests to make sure that the system was working properly. This equipment allows resistivity measurements up to 10^{17} Ω. The level of applied voltage, adapted to the expected resistivity, was in the range of 1,000 V for neat PC and samples containing up to 1 wt.% MWCNT and 100 V for samples with 2 wt.% and more MWCNT content. However, since for the more conductive samples, the accuracy of this equipment failed, samples with more than 2 wt.% MWCNT were tested using the more adequate Keithley electrometer model 6220 connected to a current source (Aligent 34401 A, 6 1/2 Digit Multimeter). For each sample, the *I–V* curve was obtained and the sample resistance was determined from the slope of the curve. The resistance was then converted to volume resistivity, ρ_v, ohm cm, using the formula

$$\rho_v = AR_v/D \tag{1}$$

where A is the contact surface area, D is the thickness of the sample, and R_v is the measured resistance. The electrical conductivity (σ) of the nanocomposites is the inverse of volume resistivity. Prior to measurements, all samples were dried for a minimum of 4 h at 120°C.

Thermal conductivity measurements

The thermal conductivity of the nanocomposite samples was determined using a Thermo electron, Thermo-Haake instrument (Thermo Fisher Scientific), by means of a *Transient Line-Source Technique* according to the ASTM D5930. A line source of heat, localized at the center of the molten specimen being tested, is at a thermal equilibrium with the specimen which is at a constant initial temperature. During the course of the measurement, a known amount of heat produced by the line source results in a heat wave propagating radially into the specimen. The rate of heat propagation is related to the thermal diffusivity of the polymer. The temperature rise of the line source varies linearly with the logarithm of time. When the temperature rise is plotted against the logarithm of time, the slope of the linear portion of the curve can be used directly to calculate the thermal conductivity of the sample using the following equation:

$$k = \frac{CQ}{4\pi \text{ Slope}} \tag{2}$$

where C is the probe constant, Q is the heat output per unit length, W/m, and k is the thermal conductivity, W/m K. Prior to measurements, all samples were dried for a minimum of 4 h at 120°C.

Results

Morphology

The morphology of melt-mixed nanocomposites was examined in terms of the nanotube dispersion and distribution. In this context, the dispersion refers to how well the nanotubes are disaggregated and separated in the form of single tubes at the nanoscale. On the other hand, the nanotubes are well distributed if single nanotubes or sets of nanotubes like bundles are uniformly dispersed within the whole matrix, even though nanotube aggregates might be observed. For these reasons, TEM was used to study the dispersion, while the distribution was investigated using SEM and AFM. Figure 1 shows schematics of a single tube (Fig. 1a), a nanotube bundle (Fig. 1b), and aggregates (Fig. 1c–e). A nanotube bundle consists of many single tubes sticking together; it can be viewed as an equivalent tube with a larger diameter having a smaller effective aspect ratio. It is worthwhile to mention that both single tubes and tube bundles can participate in the formation of a network or aggregates. Aggregates could be formed by single tubes (Fig. 1c), tube bundles (Fig. 1d), or both of them (Fig. 1e).

Figure 2 shows SEM micrographs of melt-mixed nanocomposites prepared at 210°C and 250°C. It is observed that at 210°C, the nanotubes are dispersed individually in the matrix (Fig. 2a), and the distribution at the microlevel is quiet uniform. On the other hand, examination of the micrograph of samples prepared at 250°C (Fig. 2b) shows that the nanotube distribution at the microlevel is not uniform. We observed for higher magnification that some bundles were pulled out from the matrix. These observations indicate that at 250°C, some of the nanotube bundles (not single nanotubes)

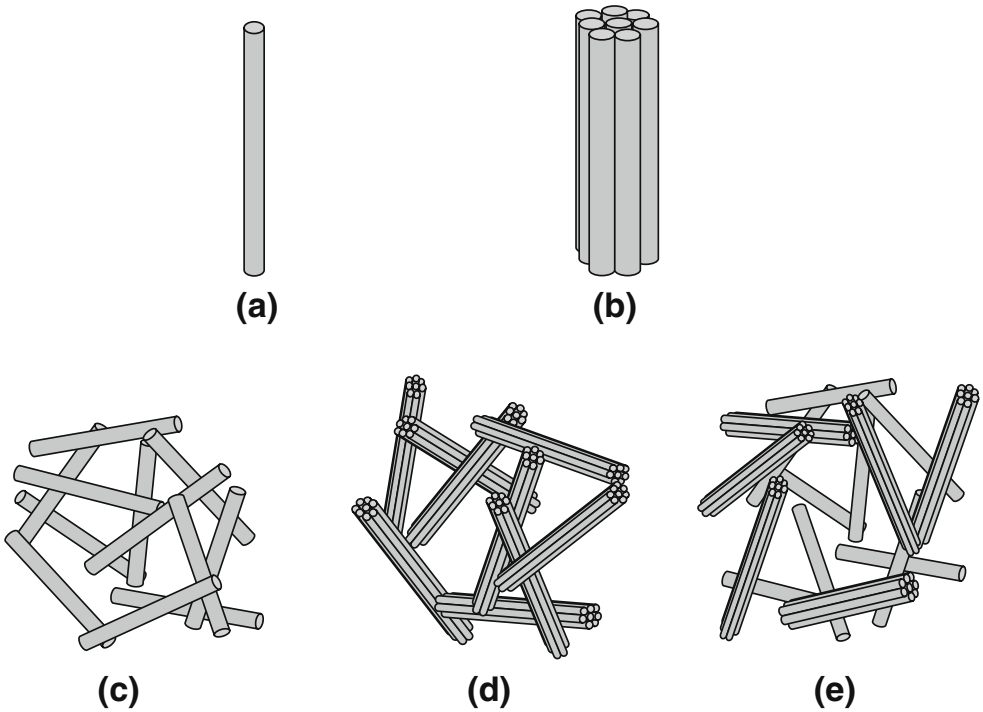

Fig. 1 Schematic figure of **a** single tube, **b** nanotube bundle, **c** aggregate of single tubes, **d** aggregate of nanotube bundles, **e** aggregate of single tube and nanotube bundles

were individually distributed and the interactions between the nanotubes, and the polymer matrix are somehow weak in this case.

The quality of the dispersion is clearly seen in the TEM photomicrographs of Fig. 3. For nanocomposites prepared at 210°C (Fig. 3a), the nanotubes are dispersed individually while at 250°C (Fig. 3b), there is no aggregates formed in the system. These results are confirmed by AFM micrographs, shown in Fig. 4a, b for samples compounded at 210°C and 250°C, respectively. As both phase and height modes show clearly, the nanotubes for the suspensions prepared at 210°C are well distributed all over the matrix without any concentrated region. This is shown clearly in the micrographs with the higher resolution on the left side. However, for the suspensions prepared at 250°C, the dispersion is not uniform: the nanotubes are concentrated in some area while there is a large region without any particles in it.

In summary, the quality of the dispersion was surprisingly better for samples prepared at 210°C. Normally, assuming that the dispersion of the nanoparticles is controlled by the diffusion, it is expected to have a better dispersion at higher temperature due to the lower viscosity of the polymer matrix. Apparently, in

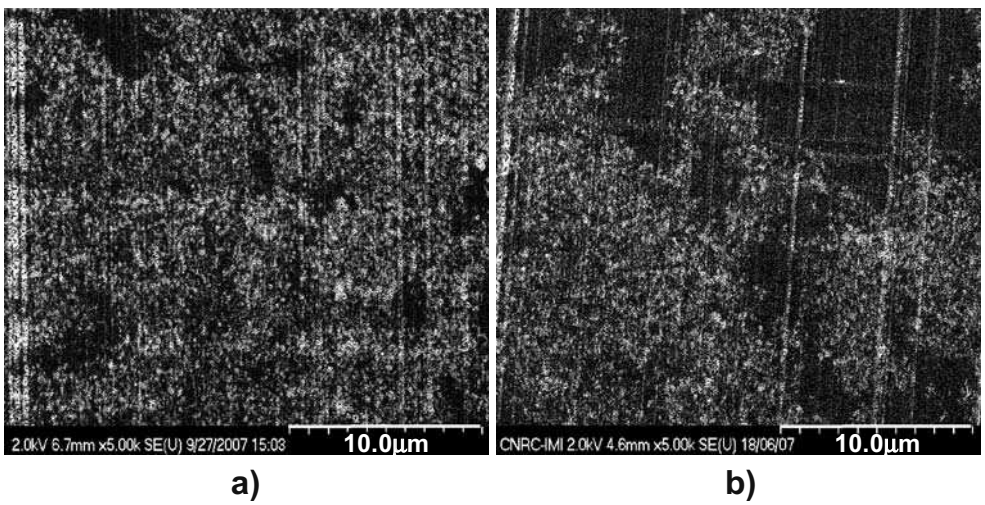

Fig. 2 SEM micrographs of ultramicrotomed surfaces of PC/5 wt.% MWCNT nanocomposites prepared at **a** 210°C and **b** 250°C

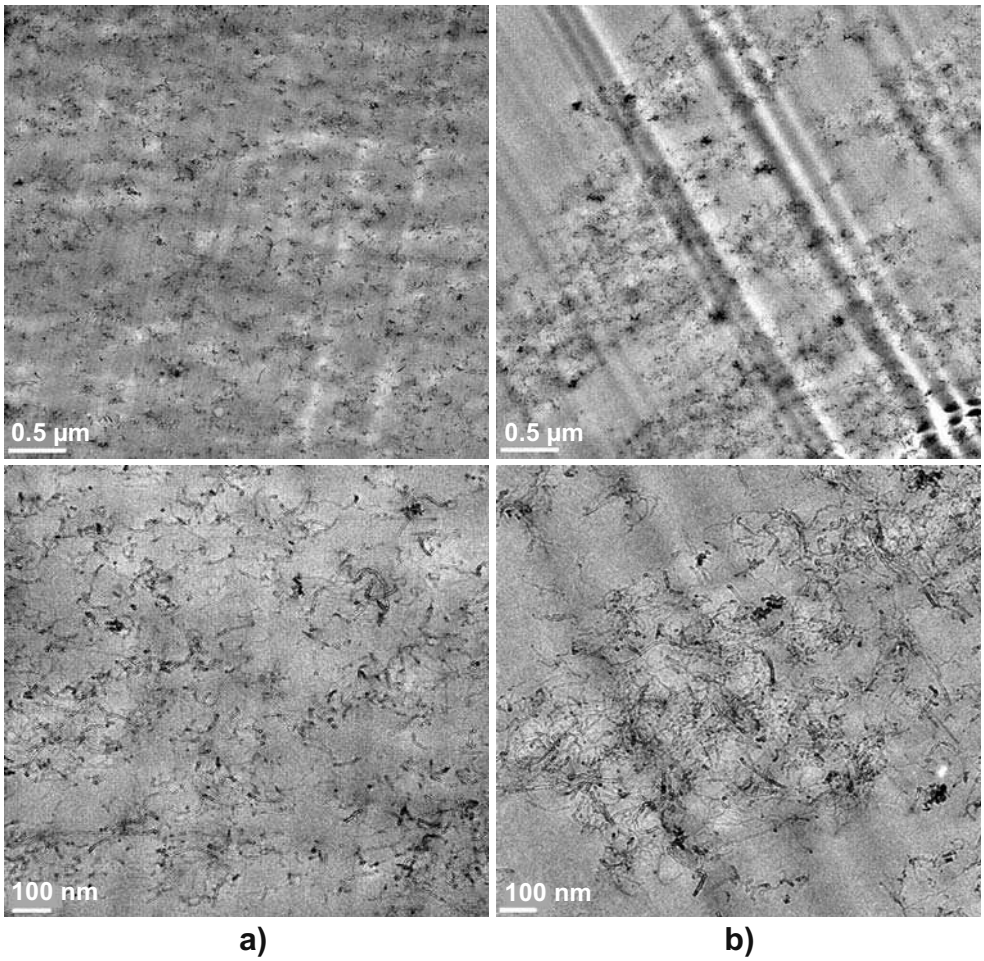

Fig. 3 TEM micrographs of PC/5 wt.% MWCNT nanocomposites prepared at **a** 210°C and **b** 250°C. The *top* and *bottom* micrographs are related to the low and high magnification, respectively

this case, the shear stress plays a more important role than the viscosity of the matrix, and the higher shear stress at the lower temperature results in a better dispersion and distribution. The main reason for this is still unclear and needs to be further investigated. For further characterization, we used the nanocomposites prepared at 210°C.

Rheological properties

The complex viscosity (η^*) and storage modulus (G') obtained from SAOS measurements at 230°C in absence of preshearing are reported in Fig. 5 for the neat PC and all nanocomposites. At low frequencies, the fully relaxed PC chains exhibit the typical Newtonian viscosity plateau. The low frequency G' data for the neat PC were not accurate enough to verify the terminal zone, $G' \propto \omega^2$. As can be seen in Fig. 5, with the addition of MWCNT, the low-frequency complex viscosity significantly increases, particularly at high loading, indicating that the long polymer chain relaxation in the nanocomposites is effectively restrained by the presence of the nanotubes. Thus, the Newtonian plateau for the viscosity disappears progressively, and a remarkable shear-thinning behavior is exhibited. The terminal behavior for the storage modulus also disappears gradually, and the dependence of G' on ω at low frequencies becomes very weak. For MWCNT loadings of 1 wt.% and above, significant jumps in the low-frequency rheological properties are observed indicating a transition from viscoelastic liquid- to solid-like behavior. In other words, with increasing filler content, nanotube–nanotube interactions begin to dominate, leading eventually to a percolation network, which restrains the long-range motion of the polymer chains. Similar rheological behavior has been observed for other polymer nanocomposites containing clays or carbon nanotubes (Du et al. 2004; Thostenson et al. 2005; Hu et al. 2006; Zhang et al. 2006; Xiao et al. 2007). As expected, the loss tangent, tanδ, where δ is the phase angle, is shown in Fig. 6 to be very sensitive to the structural change of the materials. In this figure,

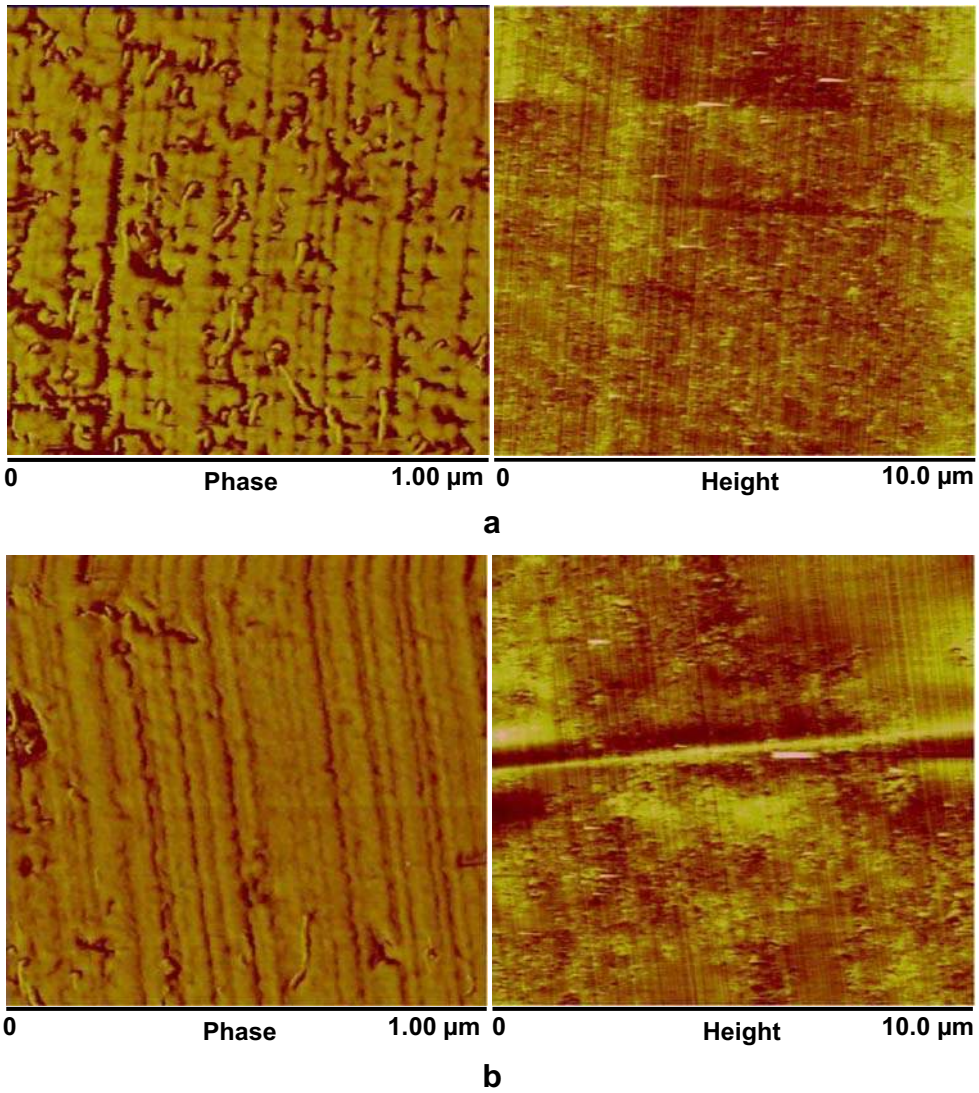

Fig. 4 AFM micrographs of PC/5 wt.% MWCNT nanocomposites prepared at **a** 210°C and **b** 250°C. The micrographs on the *left* for the phase mode are shown for the higher magnification (*scale bar* of 1 μm)

the peaks occur at the frequency of about 1 rad/s and disappear with increasing nanotube content, showing that the material becomes more elastic. This is also the characteristic of a viscoelastic material experiencing a fluid–solid transition. At the transition point, tanδ is expected to be independent of frequency.

It is also well known that an interconnected structure of anisometric filler in a polymeric matrix results in an apparent yield stress (Utracki 1986; Feldman 1987; Dealy and Wissbrun 1990; Shenoy 1999). While this effect is visible in dynamic measurements of G' and G'' versus frequency by the presence of a plateau at low frequency, it is more obvious if we plot the complex viscosity versus the complex modulus. As Fig. 7 reveals, above 1.0%t of MWCNT an apparent yield stress is observed suggested by the rapidly increasing complex viscosity as the complex modulus is decreasing.

The rheological percolation threshold was determined by using the low frequency G' data as a function of MWCNT loadings as reported in Fig. 8. As the MWCNT loading is increased up to about 1 wt.%, the low frequency G' of the nanocomposite increases by almost two orders of magnitude compared with that of the polycarbonate matrix. It can be assumed that the viscoelastic properties of the nanocomposites at low MWCNT loadings ($\leq$0.5 wt.%) are still dominated by the polycarbonate matrix. With increasing MWCNT loading, the nanocomposites experience a transition from liquid-like behavior to solid-like one, and the results suggest that the rheological percolation threshold for this system is between 0.5 and 1 wt.%. The percolation threshold is defined as the value of the solid content above which the rheological properties increase in an exponential way. This value can

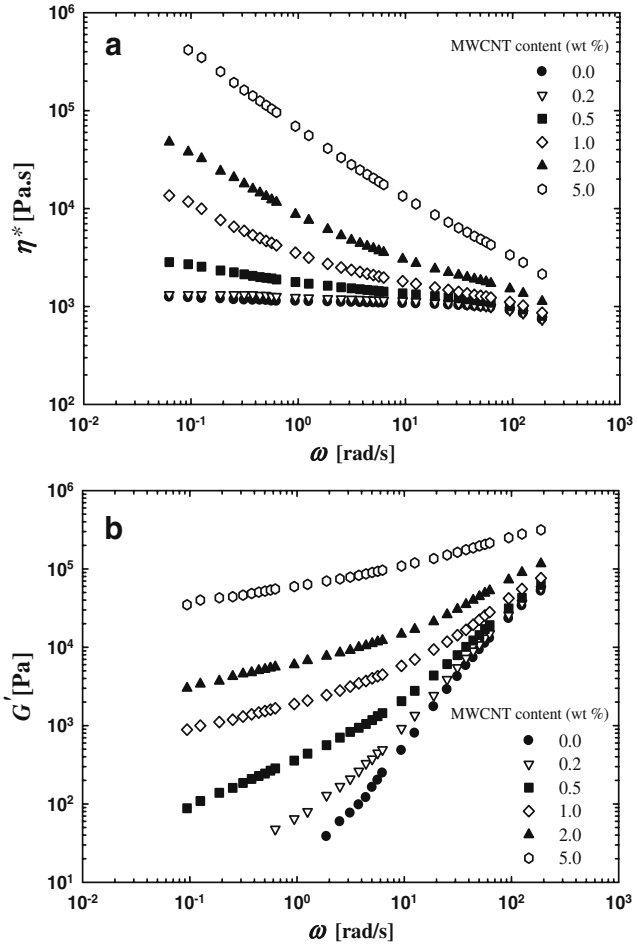

Fig. 5 **a** Complex viscosity and **b** storage moduli of polycarbonate/MWCNT as a function of frequency at 230°C

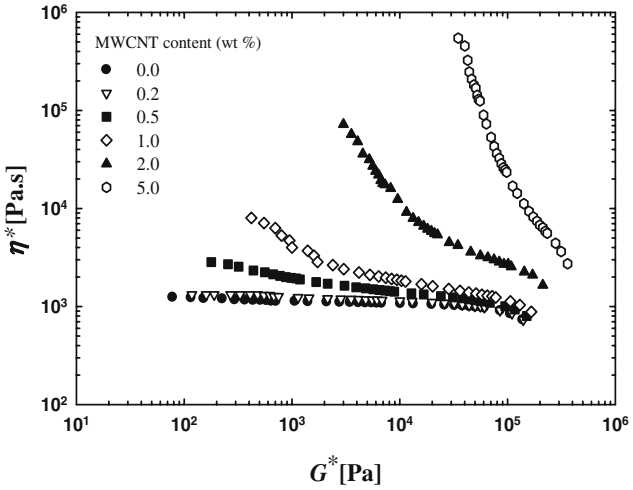

Fig. 7 Plots of η^* versus G^* for the apparent yield stress in polycarbonate/MWCNT nanocomposites at 230°C

be determined by applying a power-law function to the G' versus nanotube loading according to the following equation (Du et al. 2004; Moniruzzaman and Winey 2006):

$$G' = \beta_{cG}\left(\frac{m - m_{cG}}{m_{cG}}\right)^{n} \quad \text{for } m > m_{cG} \tag{3}$$

where β_{cG} and n are power-law constants, m is nanotube loading (wt.%) and m_{cG} is the percolation threshold (wt.%). The description of the data by Eq. 3 is shown in Fig. 8 to be very good after percolation point (as the definition of the equation suggests it can fit only the data beyond the percolation threshold). The left

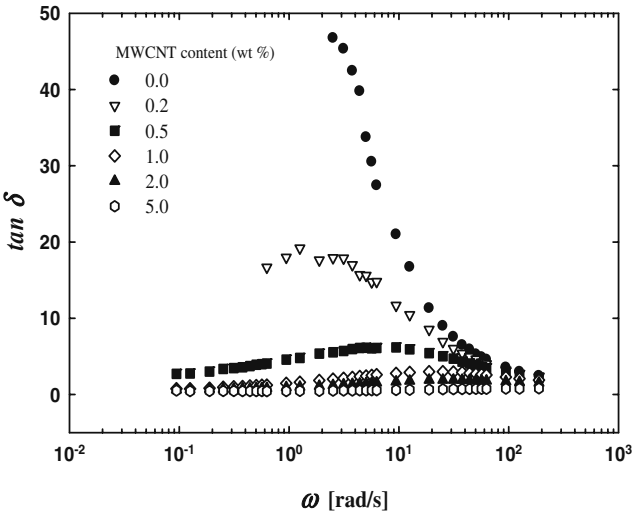

Fig. 6 tan δ of polycarbonate/MWCNT as functions of the frequency at 230°C

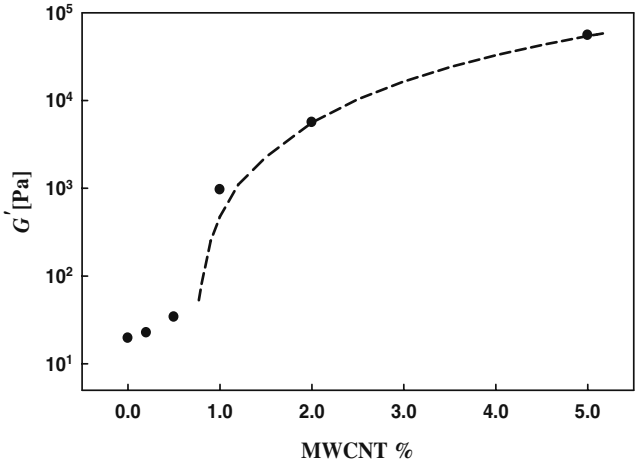

Fig. 8 Storage modulus, G', of the polycarbonate/MWCNT nanocomposite as a function of the nanotube loading at 230°C (1 rad/s data). The *line* is a fit with the power-law expression (Eq. 3)

limit of the dashed line corresponds to the percolation threshold value of 0.66 wt.% at 230°C.

Temperature effect

The results presented above are for measurements carried out at 230°C. Although the same behavior was observed for all temperatures studied, the effect of MWCNT loading was significantly different. The differences in the viscoelastic behavior as a function of temperature are better observed by using the so-called Cole–Cole plots (Friedrich and Braun 1992; Ivanov et al. 2001). In fact, analogous to Cole–Cole plots used in dielectric spectroscopy (Cole and Cole 1941; Havriliak 1997), the real and imaginary components of viscoelastic properties are plotted against each other in such a representation. A regular semi-arc is obtained if the deformation behavior of the material can be described by a single relaxation time or a narrow distribution; however, in complex polymeric systems, processes with more than one relaxation time take place leading to the distortion of the arc or to the appearance of a second arc. Such plots were used to investigate the microstructure or molecular architecture of homopolymers or materials with a wide relaxation time distribution such as heterogeneous polymeric systems like block copolymers and polymer blends (Harrell and Nakajima 1984; Chopra et al. 2002). In this study, we used Cole–Cole plots to investigate temperature induced changes in the microstructure of nanocomposites and the results are reported in Fig. 9 for two different temperatures, 210°C and 300°C, which are the two limits of our measurement temperature range. It can be observed clearly that at 210°C (Fig. 9a), the neat polycarbonate and the nanocomposites containing low MWCNT loading present a single relaxation arc. This indicates that the presence of the MWCNT has almost no influence on the relaxation behavior of the PC, and the rheological characteristics of the matrix dominate the behavior of the composites. However, at contents of 0.5 wt.% and above, all plots are partitioned into two regions: a semicurved arc at low viscosities corresponding to the local dynamics of polycarbonate chains and a linear or rigid end at higher viscosity related to the long-term relaxation of nanotubes. At higher MWCNT loadings, the first region progressively disappears, and the linear region dominates the plots suggesting that the long-range motion of polymer chains is drastically restrained. At 300°C (Fig. 9b), however, these changes are more significant. To illustrate the effects for the low-concentration nanocomposites, an insert for the low viscosity values is presented inside Fig. 9b. Even for the 0.2 wt.% nanocomposite,

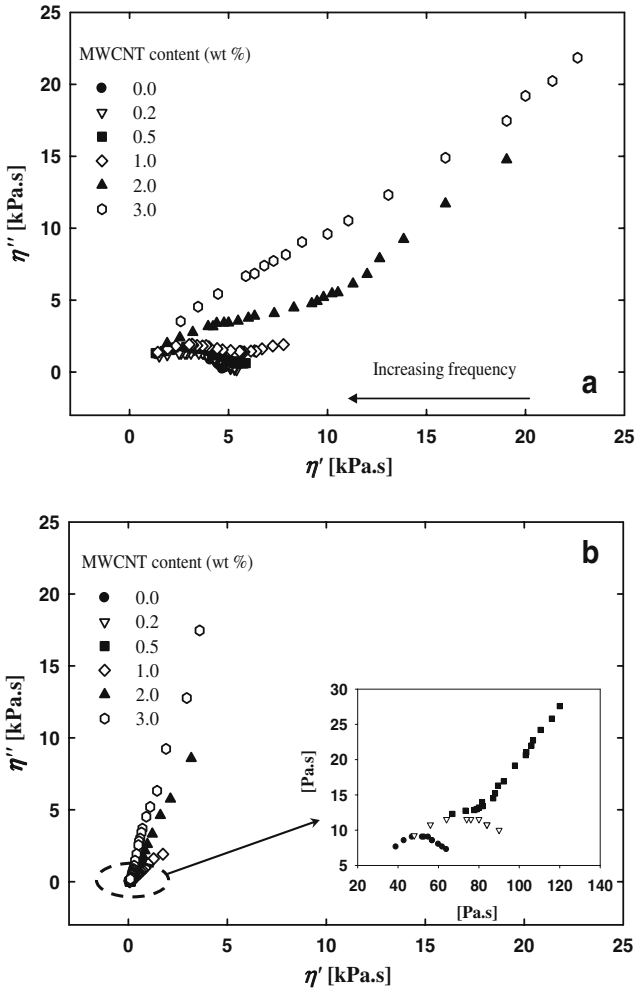

Fig. 9 Cole–Cole plots of imaginary viscosity (η'') versus real viscosity (η') for polycarbonate/MWCNT nanocomposites at **a** 210°C **b** 300°C

the Cole–Cole plot deviates from that of homogeneous polymeric materials suggesting that at higher temperature nanotube networks might be formed at a very low loading. The slopes of the linear or rigid ends of the plots are also significantly steeper, which reveals that the effect of nanotubes on the nanocomposite structure and properties is considerably enhanced at higher temperature.

To investigate the effect of temperature in more details, the rheological percolation thresholds of the nanocomposites (calculated from low frequency (1 rad/s) G' versus MWCNT loading and Eq. 3) are plotted versus the measurement temperature in Fig. 10. As this graph shows clearly the percolation threshold is very sensitive to temperature, decreasing considerably as the temperature rises; however, when the measurement temperature is high enough, the percolation threshold tends to reach a plateau. Such a temperature

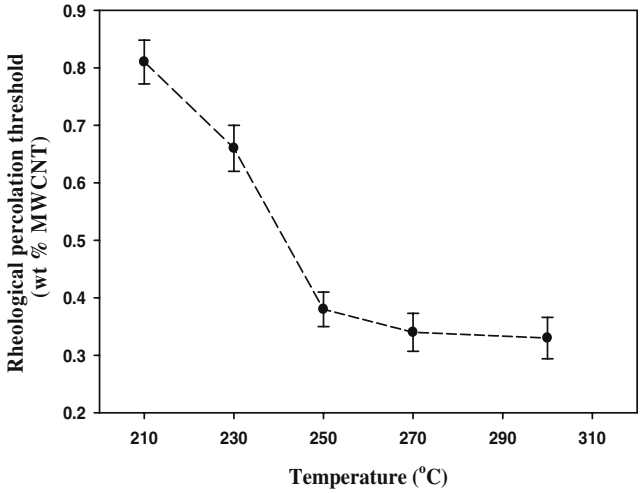

Fig. 10 Effect of temperature on the rheological percolation threshold of polycarbonate/MWCNT nanocomposites

dependency of the rheological percolation threshold has been established before in the literature (Abdel-Goad et al. 2004; Wu et al. 2007b), and it is in agreement with the trend shown by the Cole–Cole plots of Fig. 9.

Figure 11 shows the effect of temperature on the reduced complex viscosity of the nanocomposites as a function of loading for different temperatures. By dividing the complex viscosity of the nanocomposites by that of the matrix at the same temperature, the reduced data show clearly the effect of temperature on the particle–particle interactions. Of great interest are the significant increases of the reduced viscosity of the nanocomposites as the temperature rises, the effect being more pronounced at larger MWCNT content. Therefore, contrarily to expectations, nanotube–nanotube interactions increase significantly with temperature particularly at larger MWCNT content. This could also suggest that the wettability of PC by the carbon nanotubes decreases as the temperature increases, resulting in the formation of large aggregates.

The nanotube network can be considered to be an elastic structure and the strength of such a network can be related to the cohesion energy, which is the work required to break up the elastic structure (Bossard et al. 2007; Chougnet et al. 2007). The cohesive energy per volume unit, E_C, can be defined by

$$E_C = 0.5\gamma_C^2 G' \tag{4}$$

where γ_C is the critical deformation amplitude for the limit of the linear domain. Figure 12 reports the storage modulus of the nanocomposite containing 3 wt.% MWCNT as a function of the strain amplitude for temperatures ranging from 210°C to 300°C. Basically, the linear domain is limited to very low deformation, where the storage modulus G' is constant. The linear domain for the loss modulus (data not shown) is much wider. In this work, γ_C is taken as the value for which the storage modulus is equal to 95% of the plateau value. Table 1a reports the γ_C values for different temperatures of the nanocomposites containing 3 wt.% MWCNT. The values for G' and G'' in the linear regime at 1 Hz, a characteristic elastic time λ and the cohesive energy can be also found in this table. As we expected, the cohesion energy increases with temperature. The cohesive energy is representative of the network strength, and accordingly, its increase is a direct consequence of the

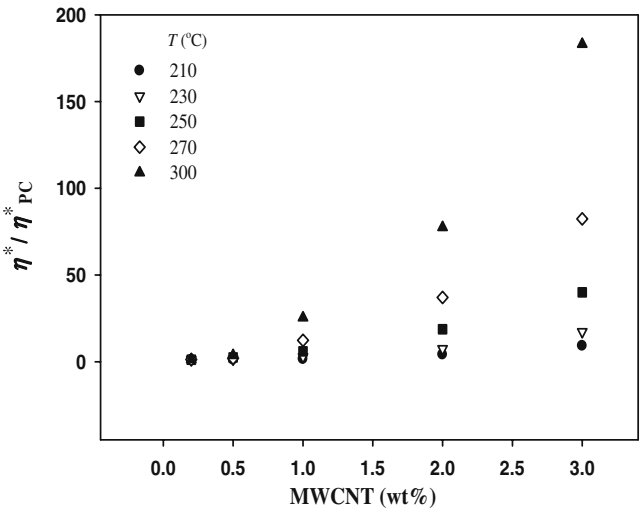

Fig. 11 Effect of temperature on reduced viscosity of polycarbonate/MWCNT nanocomposites (1 rad/s data)

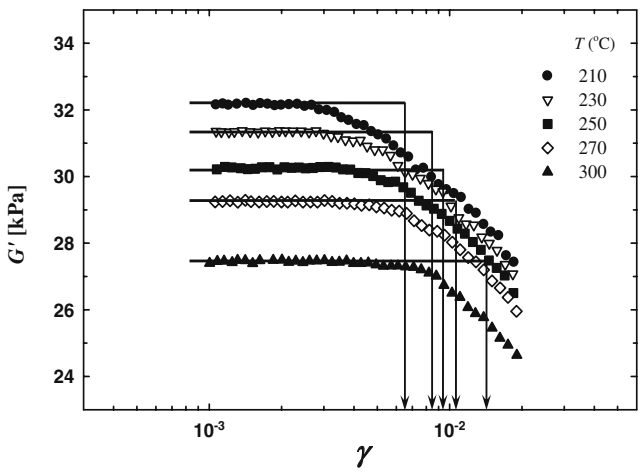

Fig. 12 Storage modulus of PC/3 wt.% MWCNT nanocomposites as a function of the strain amplitude

Table 1 Key characteristics of nanocomposites. (G' and G'' data for $\omega = 6.28$ rad/s, $\gamma < \gamma_C$, the elastic characteristic time λ, and the cohesive energy E_C)

	G' (kPa)	G'' (kPa)	$\lambda = G'/G''\omega$ (s)	γ_C	$E_C = 0.5\gamma_C^2 G'$ (mJ/m^3)
(a) Nanocomposite PC/3 wt.% MWCNT at different temperatures					
T(°C)					
210	30.4	53.6	0.090	0.0067	0.67
270	27.6	12.2	0.359	0.0119	1.95
300	25.1	8.8	0.457	0.0161	3.26
(b) Nanocomposites PC/MWCNT with different nanotube contents at 270°C					
MWCNT content (wt.%)					
0.20	79	1659	0.008	0.0318	0.04
1.0	1875	2997	0.100	0.0150	0.21
3.0	27569	12223	0.359	0.0119	1.95

enhancement of nanotube–nanotube interactions (and stronger networks) at higher temperature. The effect of nanotube concentration was also examined in the same manner. The key characteristics of the nanocomposites with different nanotube loadings at temperature of 270°C are reported in Table 1b. The cohesive energy increases with nanotube content indicating that the nanotube interactions (and networks) are stronger at higher loading level.

Orientation effect

It is widely accepted that shearing tends to align the particles in the flow direction, reducing markedly the particle–particle interactions and leading to a remarkable change of viscoelastic behavior (Fan and Advani 2007). It was observed that rod-like nanotubes are oriented easily along the shear direction and that the percolation network of nanotubes is quite sensitive to steady shear flow (Wu et al. 2007a). In order to investigate the effect of orientation on the PC/MWCNT rheological behavior, we measured the percolation thresholds in SAOS after applying different levels of stresses as preshearing steps. We first determined the shear stresses for which the nanocomposite response changes from solid- to liquid-like using plots of the steady shear stress versus shear rate of Fig. 13. These values are indicated by the arrows in the figure. However, these critical points are not clear for the low nanotube content suspensions and should not be interpreted as apparent yield stress values.

For each concentration, the samples were presheared at two levels of shear stresses: the maximum allowable stress of the CSM rheometer (2,400 Pa) as the high stress level and the stress value corresponding to the transition shown in Fig. 13 as the low stress value. Note that preshearing at lower stresses than the minimum values shown in the figure did not affect subsequent SAOS measurements. As soon as the preshearing step was completed (i.e., the shear viscosity has reached steady state), SAOS tests were conducted without any rest time. Figure 14 shows the effect of preshearing on the complex viscosity of the neat polycarbonate and nanocomposites containing 0.2 and 3 wt.% of MWCNT at 300°C. Obviously, for the neat polycarbonate and the 0.2 wt.% nanocomposites, the effect of preshearing is negligible, which indicates that the viscoelastic behavior is dominated by the polymer matrix. However, for nanocomposites with high nanotube loadings, the effect of preshearing becomes quite significant. Applying a shear flow prior to SAOS measurements, even at the low stress level, aligns the nanotubes in the flow direction and results in a lower complex viscosity. Consequently, the nanotubes interconnect minimally leading to a remarkable increase in the percolation threshold as one can deduce from Fig. 15 that reports the elastic modulus data as a function of nanotube content for different shear levels or

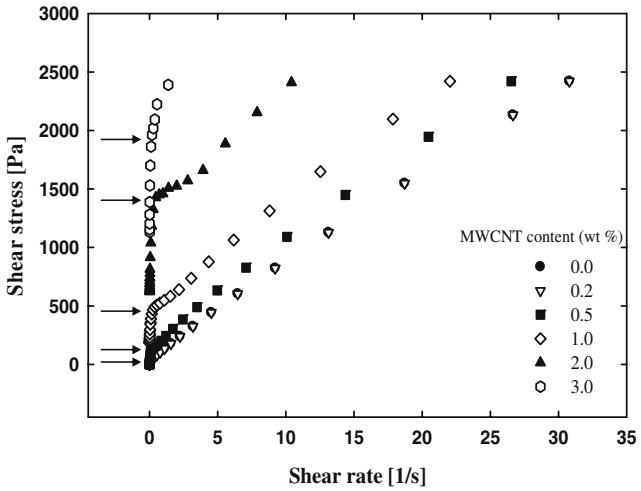

Fig. 13 Steady shear stress versus shear rate of PC/MWCNT nanocomposites at 300°C. The *arrows* show the apparent yield stress of the nanocomposites

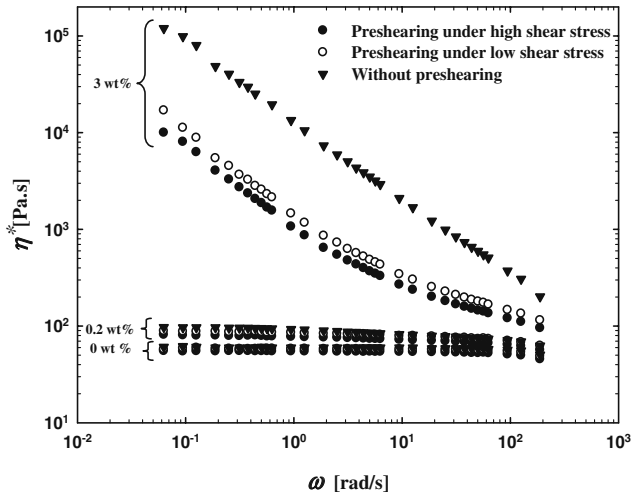

Fig. 14 Effect of preshearing (without rest time) on the complex viscosity at 300°C of nanocomposites with various nanotube loadings

no preshearing. Furthermore, this figure reveals that the storage modulus at 300°C increases very little with nanotubes concentration after preshearing under both low and high stresses, suggesting that we do not have a percolated network anymore, even at high nanotubes content. Interestingly, Fig. 15b, c shows that at lower temperature, the decrease of the storage modulus is much less sensitive to preshearing; at 250°C, we still have percolated networks even after applying high levels of stress. The results of Fig. 15 suggest that the nanotubes become more rigid and align more easily in a shear flow as the temperature is increased.

Discussion

To our knowledge, no rheological model exists to predict the strong temperature dependency of the particle interactions as observed in this work. In this section, we consider the nanocomposite system as a viscous suspension of a rod-like filler to get at least a qualitative explanation of our experimental findings, although further experiments and theoretical consideration on the interactions between nanotubes and polymer chains as well as between the nanotubes themselves are still needed.

The viscosity of a suspension of solid particles is generally determined by the nature of interactions between the particles, which depends mainly on the filler concentration. In the case of rod-like particles, the aspect ratio is another important factor affecting the viscosity of the suspension. For a particle of length L and diameter D, the aspect ratio is defined as $P = L/D$. For suspensions of such rod-like particles, depending on the rod dimensions, three concentration regimes are considered (Shaqfeh and Fredrickson 1990):

1. Dilute regime where $\phi << (D/4L)^2$
2. Semi-dilute regime where $(D/4L)^2 << \phi << (D/4L)$
3. Concentrated regime where $(D/4L) << \phi$

where ϕ is the volume fraction.

In the dilute regime, the particle interactions are almost negligible. In the semi-dilute regime, the particles interact mostly through long-range hydrodynamic interaction. If additional non-hydrodynamic interactions become important, then we have a concentrated suspension.

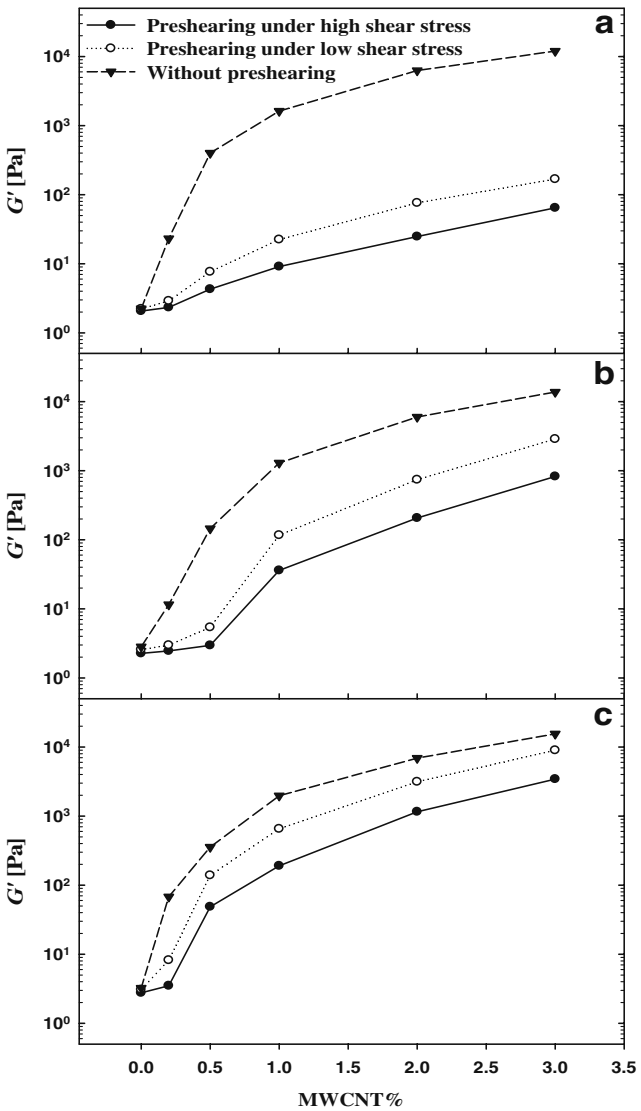

Fig. 15 Effect of preshearing (without rest time) on G' data (1 rad/s): **a** 300°C, **b** 270°C, **c** 250°C

The particles in our system are MWCNT with a diameter ranging from 15 to 50 nm and the lengths between 1 and 10 μm. The nanotube concentrations in the nanocomposites are between 0.2 to 3 wt.%, which correspond to the volume fractions of about 0.14 to 2 vol.% of MWCNT, considering the density of nanotubes to be 1.75 g/mL (Potschke et al. 2002). The density of polycarbonate was evaluated at the appropriate temperature to convert the mass fraction of nanotubes to the corresponding volume fraction. Subsequently, this concentration range corresponds to semi-dilute suspensions.

The intrinsic viscosity $[\eta]$ is one of the key characteristics to measure the contribution of the individual particles to the viscosity of a suspension and can provide considerable physical insights. It is defined by the following expression (Carreau et al. 1997):

$$[\eta] = \lim_{\phi \to 0} \frac{\eta_r - 1}{\phi} = \lim_{\phi \to 0} \frac{\eta_{sp}}{\phi} \tag{5}$$

where the relative viscosity, η_r is the ratio of the suspension viscosity to the medium viscosity and η_{sp} is the specific viscosity. In our case, however, instead of using the suspension shear viscosity, we considered the complex viscosity and the intrinsic viscosity was then determined at each temperature by extrapolating the values of the specific complex viscosity/volume fraction to zero concentration as shown in Fig. 16. The extrapolation is done assuming a linear behavior at the lowest concentrations and only two data could be used for the higher temperature measurements. The intrinsic viscosity values are listed in Table 2 for several temperatures. Interestingly, the intrinsic viscosity value increases from 15°C at 210°C to 180°C at 300°C. These values are rationalized in the following paragraphs.

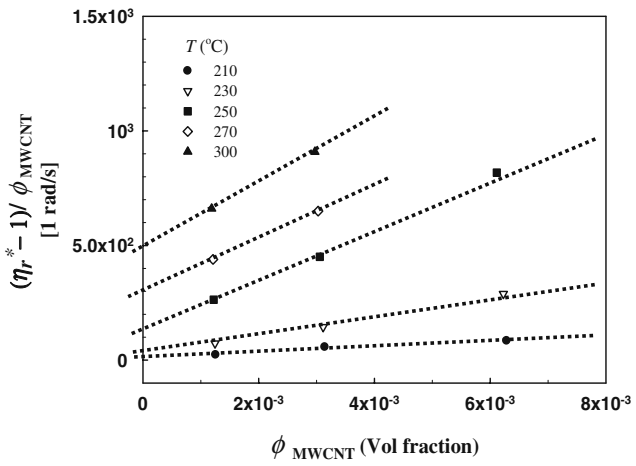

Fig. 16 Specific viscosity/volume fraction of the nanocomposites as a function of volume fraction at different temperatures

Table 2 Intrinsic viscosity of the nanocomposites and effective aspect ratio of nanotubes at different temperatures

T(°C)	210	270	300
$[\eta]$	15 ± 2	300 ± 7	500 ± 9
P_{eff}	25	151	205

It is well established that the intrinsic viscosity is strongly dependent on the particle asymmetry. For rod particles, the intrinsic viscosity is related to the aspect ratio as (Barnes et al. 1989):

$$[\eta] = 7P^{5/3}/100 \tag{6}$$

Equation 6 was used to calculate the aspect ratios corresponding to the different temperature measurements and the results are reported in Table 2. We call this an effective aspect ratio, P_{eff}, since the suspensions probably form bundles of nanotubes as suggested by the low values reported in Table 2 for low temperature (the nominal aspect of the individual nanotubes should be between 20 and 666). P_{eff} is shown to increase from 25 for the lowest temperature measurements to 205 for 300°C, indicating that at higher temperatures, the bundles are more likely to be dispersed into individual nanotubes. As Fig. 1 reveals, the aspect ratio of an individual nanotube is much higher than that of a bundle. Lower percolation threshold and stronger nanotube networks at higher temperature are probably due to this effect of temperature on the effective aspect ratio of nanotubes.

On the other hand, it is well established that the intrinsic viscosity is proportional to the hydrodynamic volume of the filler. For a highly dilute suspension of hard spheres, the specific viscosity can be predicted by the Einstein equation (Larson 1998):

$$\eta_{sp} = 2.5\frac{N_B V_\eta}{V} \tag{7}$$

where N_B is the number of particles, V_η is the hydrodynamic volume of each particle, and V is total volume. According to Eq. 5, the limiting value of the specific viscosity at very low concentration is equal to $[\eta]\phi$. Obviously for rod-like particles, the proportionality constant would be different, but the increasing intrinsic viscosity with temperature could be assigned to an increase of the hydrodynamic volume of the nanotubes. In other words, the end-to-end distance of the nanotubes increases significantly with temperature suggesting that as discussed previously, the nanotubes become more rigid (strengthened out) and align more easily in a shear flow compared to nanotubes that are more flexible at lower temperature.

Table 3 Activation energy of the network formation at different nanotube loadings

MWCNT (wt.%)	0.2	1	3
E_a (kJ/mol)	74.43	20.88	16.99

Finally, to understand why the effect of temperature on the rheological properties is more pronounced at higher nanotube loading, as it was shown previously, we made use of the Andrade–Eyring equation defined for the complex viscosity as (Mendelson 1968):

$$\eta^* = B \exp\left(E_a/RT\right) \tag{8}$$

where E_a is the flow activation energy, and R is the universal gas constant. In the case of nanocomposites, E_a can be related to the interactions between polymer chains and nanotubes. The value of E_a, thus, depends on the ease with which the nanotubes move through the polymer chains. To estimate the activation energy of the nanocomposites, we have plotted the values of ln η^* (determined at 1 rad/s) as a function of $1/RT$. The activation energy is then given by the slope of this curve. Table 3 reports the values of E_a for different nanotube loadings. For the neat PC, the flow activation energy was found to be 83.9 kJ/mol in agreement with values of the literature (Van Krevelen 1990). The rapid decrease of the activation energy with increasing nanotube loading suggests that at higher nanotube loadings, the nanotubes are less restricted and have less interaction with the polymer chains; hence, less wettability with the polymer matrix and more particle–particle interactions (including all the interactions in the system between either individual nanotubes or nanotube bundles (Fig. 1)) result. A somewhat related idea was previously proposed by Dionne et al. (2006) who showed that the increasing energetic interaction between the polymer matrix and the filler with temperature increased the rate of the attachment (wetting) of the filler to the polymer according to the Arrhenius law, in which the activation energy was proportional to the polymer–nanoparticle interaction parameter.

Conductivity measurements

In the case of conductive fillers, electrical measurements are useful to understand the relationship between the rheological behavior and the nanocomposites microstructure. Figure 17 presents the effect of the nanotube loading on the conductivity of the nanocomposites. The electrical percolation threshold is between 2 and 3 wt.% of MWCNT in PC. The conductivity changes by more than 10 decades in this range of concentration and the nanocomposites with nanotube contents larger than 3 wt.% can be considered as electrically conductive. As for the rheological percolation threshold, the electrical percolation threshold can be found by applying a similar power-law expression to the electrical conductivity data (Hu et al. 2006):

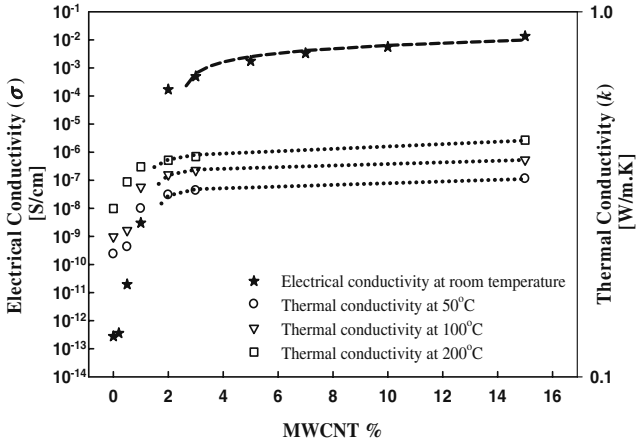

Fig. 17 Electrical conductivity (σ) and thermal conductivity (k) of the polycarbonate/MWCNT nanocomposite as a function of the nanotube loading at room temperature. The *lines* are the best fits using Eq. 9

$$\sigma = \beta_{c,\sigma}\left(\frac{m - m_{c,\sigma}}{m_{c,\sigma}}\right)^n \quad \text{for } m \geq m_{c,\sigma} \tag{9}$$

where $\beta_{c,\sigma}$ and n are power-law constants, and $m_{c,\sigma}$ is the electrical percolation threshold (wt.%). Again, this power-law expression is found to describe very well the data of Fig. 17 (after the percolation points) with an electrical percolation threshold of about 2.55 wt.%. It is worthwhile to note that rheological percolation threshold (0.66 wt.%) is considerably smaller. This difference can be described in terms of the shorter tube–tube distance required for electrical conductivity as compared to that required to impede polymer mobility, so that more nanotubes are needed to reach the electrical percolation threshold. Furthermore, all the nanotubes cannot participate in the formation of an electrically conductive path. Only metallic and semiconducting nanotubes can contribute in the electrical conductivity. Nonmetallic tubes do not have a significant contribution in electrical conductivity, although they can restrict the polymer motion.

Finally, it is well known that carbon nanotubes are thermally conductive. Hence, there must be another type of percolated structure in the nanocomposites

due to formation of a thermally conductive network. Assuming that all nanotubes are thermally conductive, the thermal conductivity percolation threshold ought to be smaller than the electrical threshold. However, the tube–tube distance required for thermal conductivity is still smaller than that required to impede polymer mobility, so that the thermal conductivity percolation threshold is expected to be higher than the rheological threshold. In addition to electrical conductivity, Fig. 17 reports the thermal conductivity of the nanocomposites as a function of MWCNT loading for a wide range of temperatures. At very low concentration of nanotubes, the thermal conductivity gradually increases with increasing nanotube content. However, at a nanotube concentration between 1 to 2 wt.%, a remarkable jump in the thermal conductivity is observed. Even though the thermal conductivity values are still much less than the corresponding values in thermally conductive materials, this stepwise change in conductivity might be due to the formation of an interconnected structure of MWCNTs and can be regarded as a thermal percolation threshold. The values of the thermal percolation threshold can be found by using the same power-law expression as for the electrical conductivity (Eq. 9). The fits are shown in Fig. 17 and the thermal conductivity percolation values are about 1.7, 1.6, and 1.47 at 50°C, 100°C, and 200°C, respectively. As we expected the thermal percolation threshold has a value between the rheological and the electrical percolation thresholds.

Concluding remarks

In this work, we have examined the effects of temperature and nanotube loading on the rheological behavior of PC/MWCNT nanocomposites. A masterbatch was diluted to prepare the nanocomposites, and a reasonably good dispersion of nanotubes within the polymer matrix was confirmed using SEM, TEM, and AFM.

Rheological measurements show that the percolation threshold and the strength of nanotube networks are significantly dependent upon the measurement temperature. Assuming that the nanotube network forms an elastic structure within the matrix, the strength of this network could be related to the cohesive energy, which is the work required to break it up. Thus, the increase of the cohesive energy with temperature is a direct consequence of the enhancement of nanotube–nanotube interactions and a stronger network at higher temperature.

The intrinsic viscosity was found to increase with temperature, and the effective aspect ratio of the nanotubes was larger at elevated temperature. This suggests that the bundle size decreases with temperature, and at higher temperature, more nanotubes are dispersed individually, and this also explains the lower percolation threshold and stronger nanotube networks at higher temperature. The increase of the intrinsic viscosity with temperature could be also due to the expansion of the nanotubes hydrodynamic volume. In other words, the end-to-end distance of the nanotubes increases significantly with temperature and results in more rigid nanotubes which align more easily under shear flow as evidenced by preshearing effects on the elastic modulus.

It was also shown that the effect of temperature is more pronounced at higher nanotube loading and can be described in terms of the activation energy of the nanocomposites. The decreasing of the activation energy with nanotube contents indicates that at higher level of loading, the interactions between the nanotubes and the polymer chains decrease. Accordingly, the nanotubes are less restricted, and their motion and interactions are more affected by temperature.

Furthermore, electrical and thermal conductivity measurements were carried out, and it was found that the formation of a conductive network above a certain content of nanotube results in an obvious jump in the conductivity (thermal and electrical) of the nanocomposites. The thermal percolation threshold was found to be between the rheological and electrical threshold.

Acknowledgement Financial support from NSERC (Natural Science and Engineering Research Council of Canada) is gratefully acknowledged. We are also thankful to Ms. Weawkamol Leelapornpisit for her great help in the morphological studies.

References

Abdel-Goad M, Potschke P (2005) Rheological characterization of melt processed polycarbonate-multiwalled carbon nanotube composites. J Non-Newton Fluid Mech 128(1):2–6

Abdel-Goad M, Potschke P, Alig I, Dudkin S, Lellinger D (2004) Rheological and dielectrical characterization of melt mixed polycarbonate-multiwalled carbon nanotube composites. Polymer 45(26):8863–8870

Barnes HA, Hutton JF, Walters K (1989) An introduction to rheology. Elsevier, Amsterdam

Bossard F, Moan M, Aubry T (2007) Linear and nonlinear viscoelastic behavior of very concentrated plate-like kaolin suspensions. J Rheol 51(6):1253–1270

Breuer O, Sundararaj U (2004) Big returns from small fibers: a review of polymer/carbon nanotube composites. Polym Compos 25(6):630–645

Carreau PJ, De Kee DCR, Chhabra RP (1997) Rheology of polymeric systems principles and applications. Hanser, New York

Chopra D, Kontopoulou M, Viassopoulos D, Hatzikiriakos SG (2002) Effect of maleic anhydride content on the rheology and phase behavior of poly(styrene-co-maleic anhydride)/poly(methyl methacrylate) blends. Rheol Acta 41(1):10–24

Chougnet A, Audibert A, Moan M (2007) Linear and non-linear rheological behaviour of cement and silica suspensions. Effect of polymer addition. Rheol Acta 46(6):793–802

Cole KS, Cole RH (1941) Dispersion and absorption in dielectrics I. Alternating current characteristics. J Chem Phys 9(4):341–351

Dealy JM, Wissbrun KF (1990) Melt rheology and its role in plastics processing: theory and applications. Van Nostrand Reinhold, New York

Ding W, Eitan A, Fisher FT, Chen X, Dikin DA, Andrews R, Brinson LC, Shadler LS, Ruoff RS (2003) Direct observation of polymer sheathing in carbon nanotube-polycarbonate composites. Nano Lett 3(11):1593–1597

Dionne PJ, Picu CR, Ozisik R (2006) Adsorption and desorption dynamics of linear polymer chains to spherical nanoparticles: a monte carlo investigation. Macromolecules 39(8):3089–3092

Du F, Scogna RC, Brand S, Fischer JE, Winey KI (2004) Nanotube networks in polymer nanocomposites: rheology and electrical conductivity. Macromolecules 37(24):9048–9055

Fan Z, Advani SG (2007) Rheology of multiwall carbon nanotube suspensions. J Rheol 51(4):585–604

Feldman D (1987) In: Ottenbrite RM, Utracki LA, Inoue S (eds) Current topics in polymer science, vol II. C Hanser Publishers, Munich, Vienna, New York, 1987, 358 pp.

Friedrich C, Braun H (1992) Generalized Cole-Cole behavior and its rheological relevance. Rheol Acta 31(4):309–322

Harrell ER, Nakajima N (1984) Modified Cole-Cole plot based on viscoelastic properties for characterizing molecular architecture of elastomers. J Appl Polym Sci 29(3):995–1010

Havriliak JS (1997) Dielectric and mechanical relaxation in materials: analysis, interpretation and application to polymers. Hanser, Munich

Hone J (2004) Carbon nanotubes: thermal properties. Dekker encyclopedia of nanoscience and nanotechnology. Dekker, New York, pp 603–610

Hong JS, Kim C (2007) Extension-induced dispersion of multiwalled carbon nanotube in non-Newtonian fluid. J Rheol 51(5):833–850

Hu G, Zhao C, Zhang S, Yang M, Wang Z (2006) Low percolation thresholds of electrical conductivity and rheology in poly(ethylene terephthalate) through the networks of multiwalled carbon nanotubes. Polymer 47(1):480–488

Iijima S (1991) Helical microtubules of graphitic carbon. Nature 354:56–58

Iijima S, Ichihashi T (1993) Single-shell carbon nanotubes of 1-nm diameter. Nature 363(6430):603–615

Ivanov I, Muke S, Kao N, Bhattacharya SN (2001) Morphological and rheological study of polypropylene blends with a commercial modifier based on hydrogenated oligo (cyclopentadiene). Polymer 42(24):9809–9817

Kharchenko SB, Migler KB, Douglas JF, Obrzut J, Grulke EA (2004) Rheology, processing and electrical properties of multiwall carbon nanotube/polypropylene nanocomposites. ANTEC 2004:1877–1881

Larson RG (1998) The structure and rheology of complex fluids. Oxford University Press, New York

Ma WKA, Chinesta F, Ammar A (2008) Rheological modeling of carbon nanotube aggregate suspensions. J Rheol 52(6):1311–1330

Meincke O, Kaempfer D, Weickmann H, Friedrich C, Vathauer M, Waeth H (2004) Mechanical properties and electrical conductivity of carbon-nanotube filled polyamide-6 and its blends with acrylonitrile/butadiene/styrene. Polymer 45(3):739–748

Mendelson RA (1968) Prediction of melt viscosity flow curves at various temperatures for some olefin polymers and copolymers. Polym Eng Sci 8(3):235–240

Meyyappan M (2005) Carbon nanotubes: science and applications. CRC, Boca Raton

Moniruzzaman M, Winey KI (2006) Polymer nanocomposites containing carbon nanotubes. Macromolecules 39(16):5194–5205

Pham GT, Park Y-B, Wang S, Liang Z, Wang B, Zhang C, Funchess P, Kramer L (2008) Mechanical and electrical properties of polycarbonate nanotube buckypaper composite sheets. Nanotechnology 19(32):325705. doi:10.1088/0957-4484/19/32/325705

Potschke P, Fornes TD, Paul DR (2002) Rheological behavior of multiwalled carbon nanotube/polycarbonate composites. Polymer 43(11):3247–3255

Potschke P, Abdel-Goad M, Alig I, Dudkin S, Lellinger D (2004a) Rheological and dielectrical characterization of melt mixed polycarbonate-multiwalled carbon nanotube composites. Polymer 45(26):8863–8870

Potschke P, Bhattacharyya AR, Janke A (2004b) Carbon nanotube-filled polycarbonate composites produced by melt mixing and their use in blends with polyethylene. Carbon 42:965–969

Rahatekar SS, Koziol KKK, Butler SA, Elliott JA, Shaffer MSP, Mackley MR, Windle AH (2006) Optical microstructure and viscosity enhancement for an epoxy resin matrix containing multiwall carbon nanotubes. J Rheol 50(5):599–610

Salvetat JP, Bonard JM, Thomson NH, Kulik AJ, Forro L, Benoit W, Zuppiroli L (1999) Mechanical properties of carbon nanotubes. Appl Phys A 69(3):255–260

Shaqfeh ESG, Fredrickson GH (1990) The hydrodynamic stress in a suspension of rods. Phys Fluids A 2:7–24

Shenoy AV (1999) Rheology of filled polymer systems. Springer, Verlag

Singh S, Pei Y, Miller R, Sundararajan PR (2003) Long-range, entangled carbon nanotube networks in polycarbonate. Adv Functional Mater 13(11):868–872

Sung YT, Han MS, Song KH, Jung JW, Lee HS, Kum CK, Joo J, Kim WN (2006) Rheological and electrical properties of polycarbonate/multi-walled carbon nanotube composites. Polymer 47(12):4434–4439

Thostenson ET, Li C, Chou T-W (2005) Nanocomposites in context. Compos Sci Technol 65(3–4):491–516

Utracki LA (1986) Flow and flow orientation of composites containing anisometric particles. Polym Compos 7(5):9

Van Krevelen DW (1990) Properties of polymers. Elsevier, Amsterdam

Wu D, Liang W, Ming Z (2007a) Rheology of multi-walled carbon nanotube/poly(butylene terephthalate) composites. J Polym Sci B 45(16):2239–2251

Wu D, Liang W, Yurong S, Ming Z (2007b) Rheological properties and crystallization behavior of multi-walled carbon nanotube/poly(ε -caprolactone) composites. J Polym Sci B 45(23):3137–3147

Xiao KQ, Zhang LC, Zarudi L (2007) Mechanical and rheological properties of carbon nanotube-reinforced polyethylene composites. Compos Sci Technol 67(2):177–182

Xie X-L, Mai Y-W, Zhou X-P (2005) Dispersion and alignment of carbon nanotubes in polymer matrix: a review. Mater Sci Eng R: Rep 49(4):89–112

Xinfeng S, Hudson JL, Spicer PP, Tour JM, Krishnamoorti R, Mikos AG (2005) Rheological behaviour and mechanical characterization of injectable poly(propylene fumarate)/single-walled carbon nanotube composites for bone tissue engineering. Nanotechnology 16(7):531–538

Yu M-F, Lourie O, Dyer MJ, Moloni K, Kelly TF, Ruoff RS (2000) Strength and breaking mechanism of multiwalled carbon nanotubes under tensile load. Science 287(5453): 637–640

Zhang Q, Rastogi S, Chen D, Lippits D, Lemstra PJ (2006) Low percolation threshold in single-walled carbon nanotube/high density polyethylene composites prepared by melt processing technique. Carbon 44(4):778–785